CHARM DALITZ ANALYSES AT BaBar*

Marco Pappagallo†

Representing the BaBar Collaboration

Institute for Particle Physics Phenomenology, Durham University
South Road, Durham, DH1 3LE, United Kingdom

(Received June 28, 2007)

Dalitz plot analyses of D^0 events reconstructed for the hadronic decay $D^0 \to \bar{K}^0 K^+ K^-$ and $D^0 \to \bar{K}^0 \pi^+ \pi^-$ are presented here. The analyses use data collected with the BaBar detector at the PEP-II asymmetric-energy e^+e^- storage rings at SLAC running at center-of-mass energies on and 40 MeV below the $\Upsilon(4S)$ resonance.

PACS numbers: 13.25.Ft, 14.40.Cs, 12.15.Hh

1. Introduction

In this paper we report the results on a study of $D^0 \to \bar{K}^0 K^+ K^-$ decay and a measurement of $a_0(980)$ meson parameters [1]. A Dalitz plot analysis of $D^0 \to \bar{K}^0 \pi^+ \pi^-$ decay is also shown [2, 3]. The latter decay plays a fundamental role in the measurement of the angles of the Unitarity Triangle. For both decays, the $\bar{K}^0$ is detected via the decay $K_S^0 \to \pi^+\pi^-$, while the decay $D^{*+} \to D^0 \pi^+$ is used to identify the flavor of the D^0 (through the charge of the slow $\pi^{\pm}$ from D^* decay) and to reduce background. All references to an explicit decay mode, unless otherwise specified, imply the use of the charge conjugate decay as well.

2. $D^0 \to \bar{K}^0 K^+ K^-$ decay and scalar mesons

Charm Dalitz plot analyses are useful in providing new information on resonances that contribute to three-body final states. They can help to

---

* Presented at The Final EURIDICE Meeting "Effective Theories of Colours and Flavours: from EURODAPHNE to EURIDICE", Kazimierz, Poland, 24–27 August, 2006.

† Affiliated to the BaBar Collaboration through University of Warwick, Coventry, CV4 7AL, United Kingdom.

enlighten old puzzles related to light meson spectroscopy, specifically to the structure of scalar mesons. The study of $D^0 \to \bar{K}^0 K^+ K^-$ decay provides a laboratory to investigate scalar mesons coupling to the $K\bar{K}$ system, in particular the $f_0(980)$ and $a_0(980)$.

2.1. Partial wave analysis of $D^0 \to \bar{K}^0 K^+ K^-$

Using 91.5 fb^{-1} of data, a $D^0 \to \bar{K}^0 K^+ K^-$ sample of 12540 events with a signal fraction of 97.3% is selected. The Dalitz plot of the $D^0 \to \bar{K}^0 K^+ K^-$ is shown in Fig. 1(a). A strong interference between the $\phi(1020)$ and a scalar meson, which is identified as mostly due to the $a_0(980)$ resonance,

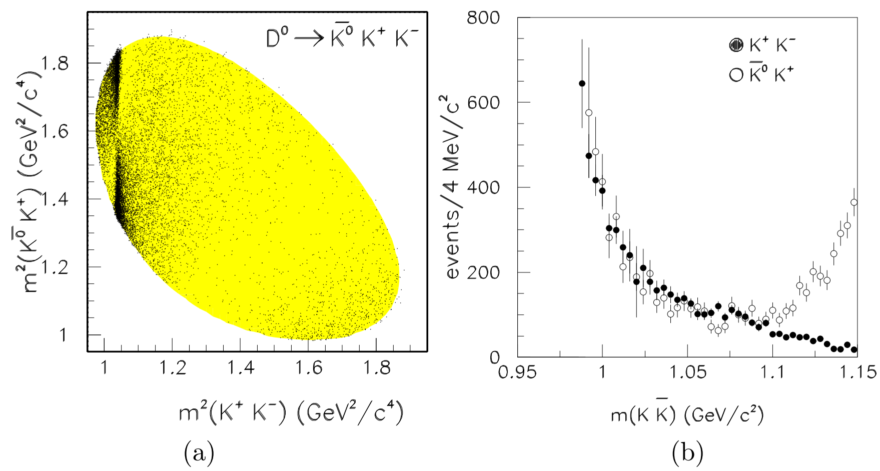

Fig. 1. (a) Dalitz plot of $D^0 \to \bar{K}^0 K^+ K^-$. (b) Comparison between the scalar K^+K^- and the $\bar{K}^0 K^+$ phase space corrected mass distributions.

is observed in the low mass $K\bar{K}$ region. The contribution of $a_0(980)^+$, in the right corner at the bottom, can also be observed. A partial wave analysis in the low mass K^+K^- region allows the K^+K^- scalar (S) and vector components (P) to be separated, thus solving the following system of equations [4]:

$$
\begin{aligned}
\sqrt{4\pi}\,\langle Y_0^0 \rangle &= S^2 + P^2\,, \\
\sqrt{4\pi}\,\langle Y_1^0 \rangle &= 2|S||P|\cos\phi_{SP}\,, \\
\sqrt{4\pi}\,\langle Y_2^0 \rangle &= \frac{2}{\sqrt{5}}P^2\,,
\end{aligned}
$$

where $\langle Y_L^0 \rangle_{L=0,1,2}$ are the efficiency corrected spherical harmonic moments. The resulting scalar K^+K^- and $\bar{K}^0 K^+$ mass distributions, corrected for phase space, are displayed in Fig. 1(b) and show a good agreement. This supports the hypothesis that the$f_0(980)$ contribution is small, since $f_0(980)$ has isospin zero and therefore cannot decay to $\bar{K}^0K^+$.

The K^+K^- S- and P-wave mass spectra, the $\bar{K}^0K^+$ mass spectrum and the phase difference ϕ_{SP} have been fit simultaneously; where the K^+K^- P-wave is supposed to be entirely due to the $\phi(1020)$ meson, the K^+K^- S-wave to the $a_0(980)^0$ and the $\bar{K}^0K^+$ mass distribution to $a_0(980)^+$, respectively. The $a_0(980)$ has been described by a coupled channel Breit–Wigner formula of the form [5]:

$$\mathrm{BW}_{\mathrm{ch}}(a_0)(m) = \frac{g_{\bar{K}K}}{m_0^2 - m^2 - i\left(\rho_{\eta\pi}g_{\eta\pi}^2 + \rho_{\bar{K}K}g_{\bar{K}K}^2\right)}\,,$$

where $g_{\eta\pi}$ and $g_{\bar{K}K}$ describe the $a_0(980)$ couplings to the $\eta\pi$ and $\bar{K}K$ systems respectively. The parameters m_0 and $g_{\eta\pi}$ have been fixed to the Crystal Barrel measurements [6] while the parameter $g_{\bar{K}K}$ has been left free in the fit. The result is (statistical error only):

$$g_{\bar{K}K} = 464 \pm 29(\mathrm{MeV})^{1/2}\,.$$

2.2. Dalitz plot analysis of $D^0 \to \bar{K}^0K^+K^-$

The $D^0 \to \bar{K}^0K^+K^-$ decay amplitude $\mathcal{A}_D(m_-^2, m_+^2)$ is expressed as a sum of two-body decay-matrix elements and a non-resonant contribution,

$$\mathcal{A}_D(m_-^2, m_+^2) = \Sigma_r a_r e^{i\phi_r}\mathcal{A}_r(m_-^2, m_+^2) + a_{\mathrm{NR}}e^{i\phi_{\mathrm{NR}}}\,,$$

where each term is parametrized with an amplitude a_r and a phase ϕ_r. The function $\mathcal{A}_r(m_-^2, m_+^2)$ is the Lorentz-invariant expression for the matrix

TABLE I

Results from the Dalitz plot analysis of $D^0 \to \bar{K}^0K^+K^-$. The fits have been performed using the value of $g_{\bar{K}K}$ resulting from the partial wave analysis.

Final state	Amplitude	Phase(radians)	Fraction(%)
$\bar{K}^0a_0(980)^0$	1.(fixed)	0.(fixed)	66.4 ± 1.6 ± 7.0
$\bar{K}^0\phi(1020)$	$0.437 \pm 0.006 \pm 0.060$	$1.91 \pm 0.02 \pm 0.10$	$45.9 \pm 0.7 \pm 0.7$
$K^-a_0(980)^+$	$0.460 \pm 0.017 \pm 0.056$	$3.59 \pm 0.05 \pm 0.20$	$13.4 \pm 1.1 \pm 3.7$
$\bar{K}^0f_0(1400)$	$0.435 \pm 0.033 \pm 0.162$	$-2.63 \pm 0.10 \pm 0.71$	$3.8 \pm 0.7 \pm 2.3$
$\bar{K}^0f_0(980)$			$0.4 \pm 0.2 \pm 0.8$
$K^+a_0(980)^-$ DCS			$0.8 \pm 0.3 \pm 0.8$
Sum			130.7 ± 2.2

element of a D^0 meson decaying into $\bar{K}^0K^-K^+$ through an intermediate resonance r, parametrized as a function of position in the Dalitz plane. We refer to this model as the Breit–Wigner (or Isobar) model [7, 8]. By an unbinned maximum likelihood fit, the $D^0 \to \bar{K}^0K^+K^-$ decay results to be dominated by $D^0 \to \bar{K}^0a_0(980)^0$, $D^0 \to \bar{K}^0\phi(1020)$ and $D^0 \to K^-a_0(980)^+$ decays (Table I). The $f_0(980)$ and the doubly Cabibbo suppressed(DCS) contributions are consistent with zero. A scalar contribution, not consistent with being uniform, is also present. It can be described by the tail of a broad resonance, the $f_0(1370)$. The $D^0 \to \bar{K}^0K^+K^-$ Dalitz plot projections together with the fit results are shown in Fig. 2.

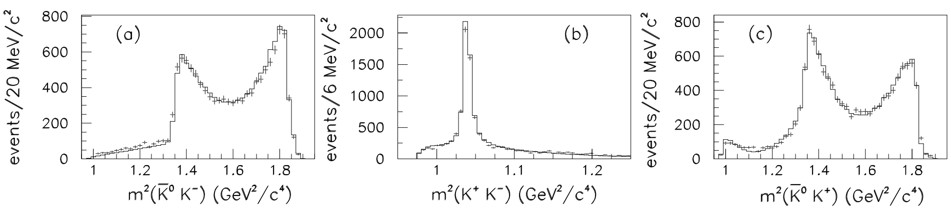

Fig. 2. Dalitz plot projections for $D^0 \to \bar{K}^0K^+K^-$ decay. The data are represented with error bars; the histograms are the projections of the fit described in the text.

3. CKM angles and the $D^0 \to K^0_S\pi^+\pi^-$ decay

Various methods have been proposed to extract the angle γ and $\cos\beta$ of the Unitarity Triangle using $B^- \to \tilde{D}^0K^-$ [9] and $B^0 \to \tilde{D}^0h^0(h^0 = \pi^0, \eta, \eta'$ or $\omega)$ [10] decays respectively, when the D^0 and $\bar{D}^0$ are reconstructed in a common final state. The symbol $\tilde{D}^0$ indicates either a D^0 or a $\bar{D}^0$ meson. Among the $\tilde{D}^0$ decay modes studied so far the $K^0_S\pi^-\pi^+$ channel is the one with the highest sensitivity because of the best overall combination of branching ratio magnitude, D^0–$\bar{D}^0$ interference and background level.

3.1. Dalitz plot analysis of $D^0 \to K^0_S\pi^+\pi^-$

A $D^0 \to K^0_S\pi^+\pi^-$ sample of 390328 events with a signal fraction of 97.7% is reconstructed in 270 fb^{-1} of data.

Table II summarizes the values of the complex amplitudes $a_re^{i\phi_r}$ obtained using a Breit–Wigner model consisting of 16 two-body elements comprising doubly Cabibbo suppressed contribution, and accounting for efficiency variations across the Dalitz plane and the small background contribution. We find that the inclusion of the scalar $\pi\pi$ resonances σ and σ' significantly improves the quality of the fit (Fig. 3)[1].

[1] The σ and σ' masses and widths are determined from the data. We find (in MeV/c^2) $M_\sigma = 490\pm6$, $\Gamma_\sigma = 406\pm11$, $M_{\sigma'} = 1024\pm4$, and $\Gamma_{\sigma'} = 89\pm7$. Errors are statistical.

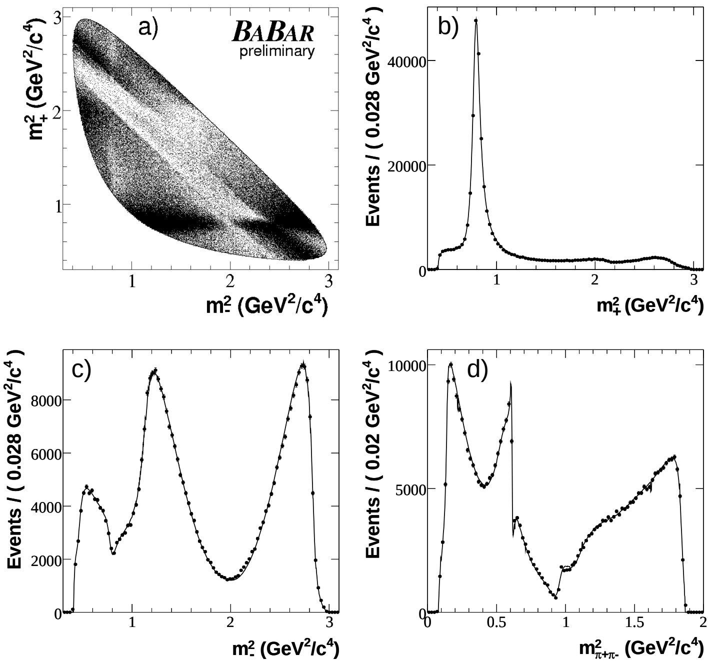

Fig. 3. (a) The $D^0 \to K^0_S\pi^-\pi^+$ Dalitz distribution. m^2_- and m^2_+ are the squared invariant masses of the $K^0_S\pi^-$ and $K^0_S\pi^+$ combinations respectively. (b) Dalitz plot projections on m^2_-, (c) m^2_+, and (d) $m^2_{\pi^+\pi^-}$. The curves are the projections of a fit using an isobar model.

3.2. Dalitz plot analysis of $D^0 \to K^0_S\pi^+\pi^-$ parametrizing the $\pi\pi$ S-wave by a K-matrix model

The K-matrix approach provides a direct way of imposing the unitarity constraint that is not guaranteed in the case of the Breit–Wigner model [11–13]. Therefore, the K-matrix method is suited to the study of broad and overlapping resonances in multi-channel decays, solving the main limitation of the Breit–Wigner model to parametrize the $\pi\pi$ S-wave states in $D^0 \to K^0_S\pi^-\pi^+$.

The Dalitz amplitude $\mathcal{A}_D(m^2_-, m^2_+)$ is written in such a case as a sum of two-body decay matrix elements for the spin-1, spin-2 and $K\pi$ spin-0 resonances (as in the Breit–Wigner model), and the $\pi\pi$ spin-0 piece denoted as F_1 is written in terms of the K-matrix. Therefore we have:

$$\mathcal{A}_D(m^2_-, m^2_+) = F_1(s) + \Sigma_{r\neq\pi\pi\,\mathrm{S-wave}} a_r e^{i\phi_r}\mathcal{A}_r(m^2_-, m^2_+)\,.$$

TABLE II

Complex amplitudes $a_r e^{i\phi_r}$ and fit fractions of the different components obtained from an isobar model fit of the $D^0 \to K_S\pi^-\pi^+$ Dalitz distribution. Errors are statistical only. The sum of fit fractions is 119.5%.

Component	$\mathrm{Re}\{a_r e^{i\phi_r}\}$	$\mathrm{Im}\{a_r e^{i\phi_r}\}$	Fit fraction (%)
$K^*(892)^-$	-1.223 ± 0.011	1.3461 ± 0.0096	58.1
$K_0^*(1430)^-$	-1.698 ± 0.022	-0.576 ± 0.024	6.7
$K_2^*(1430)^-$	-0.834 ± 0.021	0.931 ± 0.022	3.6
$K^*(1410)^-$	-0.248 ± 0.038	-0.108 ± 0.031	0.1
$K^*(1680)^-$	-1.285 ± 0.014	0.205 ± 0.013	0.6
$K^*(892)^+$ DCS	0.0997 ± 0.0036	-0.1271 ± 0.0034	0.5
$K_0^*(1430)^+$ DCS	-0.027 ± 0.016	-0.076 ± 0.017	0.0
$K_2^*(1430)^+$ DCS	0.019 ± 0.017	0.177 ± 0.018	0.1
$\rho(770)$	1	0	21.6
$\omega(782)$	-0.02194 ± 0.00099	0.03942 ± 0.00066	0.7
$f_2(1270)$	-0.699 ± 0.018	0.387 ± 0.018	2.1
$\rho(1450)$	0.253 ± 0.038	0.036 ± 0.055	0.1
Non-resonant	-0.99 ± 0.19	3.82 ± 0.13	8.5
$f_0(980)$	0.4465 ± 0.0057	0.2572 ± 0.0081	6.4
$f_0(1370)$	0.95 ± 0.11	-1.619 ± 0.011	2.0
σ	1.28 ± 0.02	0.273 ± 0.024	7.6
σ'	0.290 ± 0.010	-0.0655 ± 0.0098	0.9

TABLE III

Complex amplitudes $a_r e^{i\phi_r}$ and fit fractions of the different components obtained from a K-matrix model fit of the $D^0 \to K_S^0\pi^-\pi^+$ Dalitz distribution. Errors are statistical only. The sum of fit fractions is 116%.

Component	$\mathrm{Re}\{a_r e^{i\phi_r}\}$	$\mathrm{Im}\{a_r e^{i\phi_r}\}$	Fit fraction (%)
$K^*(892)^-$	-1.159 ± 0.022	1.361 ± 0.020	58.9
$K_0^*(1430)^-$	2.482 ± 0.075	-0.653 ± 0.073	9.1
$K_2^*(1430)^-$	0.852 ± 0.042	-0.729 ± 0.051	3.1
$K^*(1410)^-$	-0.402 ± 0.076	0.050 ± 0.072	0.2
$K^*(1680)^-$	-1.00 ± 0.29	1.69 ± 0.28	1.4
$K^*(892)^+$ DCS	0.133 ± 0.008	-0.132 ± 0.007	0.7
$K_0^*(1430)^+$ DCS	0.375 ± 0.060	-0.143 ± 0.066	0.2
$K_2^*(1430)^+$ DCS	0.088 ± 0.037	-0.057 ± 0.038	0.0
$\rho(770)$	1 (fixed)	0 (fixed)	22.3
$\omega(782)$	-0.0182 ± 0.0019	0.0367 ± 0.0014	0.6
$f_2(1270)$	0.787 ± 0.039	-0.397 ± 0.049	2.7
$\rho(1450)$	0.405 ± 0.079	-0.458 ± 0.116	0.3
β_1	-3.78 ± 0.13	1.23 ± 0.16	—
β_2	9.55 ± 0.20	3.43 ± 0.40	—
β_4	12.97 ± 0.67	1.27 ± 0.66	—
f_{11}^{prod}	-10.22 ± 0.32	-6.35 ± 0.39	—
sum of $\pi^+\pi^-$ S-wave			16.2

Table III summarizes the values of $F_1(s)$ free parameters β_α and f_{11}^{prod}, together with the spin-1, spin-2, and $K\pi$ spin-0 amplitudes as in the Breit–Wigner model. There is no overall improvement in the two-dimensional χ^2 test compared to the Breit–Wigner model since it is dominated by the P-wave components, which are identical in both models. Nevertheless, it should be emphasized that the main advantage in using a K-matrix parametrization instead of a sum of two-body amplitudes to describe the $\pi\pi$ S-wave is that it provides a more adequate description of the complex dynamics in the presence of overlapping and many channel resonances.

The contribution to the systematic uncertainties of CKM angles due to the description of the $\pi\pi$ S-wave in $D^0 \to K_S^0\pi^-\pi^+$, evaluated using a K-matrix formalism, is found to be small [2, 3].

The author is grateful for the extraordinary contributions of our PEP-II colleagues in achieving the excellent luminosity and machine conditions that have made this work possible. The collaborating institutions wish to thank SLAC for its support and kind hospitality. This work is supported by DOE and NSF (USA), NSERC (Canada), IHEP (China), CEA and CNRS-IN2P3 (France), BMBF and DFG (Germany), INFN (Italy), FOM (The Netherlands), NFR (Norway), MIST (Russia), and PPARC (United Kingdom). Individuals have received support from CONACyT (Mexico), the A.P. Sloan Foundation, the Research Corporation, and the Alexander von Humboldt Foundation. The author acknowledges the support of the EU-RTN Programme, Contract No. HPRN-CT-2002-00311, "EURIDICE".

REFERENCES

[1] B. Aubert *et al.* [BaBar Collab.], *Phys. Rev.* **D72**, 052008 (2005).

[2] B. Aubert *et al.* [BaBar Collab.], `hep-ex/0607104`.

[3] B. Aubert *et al.* [BaBar Collab.], `hep-ex/0507101`.

[4] S.U. Chung, *Phys. Rev.* **D56**, 7299 (1997).

[5] S.M. Flatte, *Phys. Lett.* **B63**, 224 (1976).

[6] A. Abele *et al.*, *Phys. Rev.* **D57**, 3860 (1998).

[7] S. Kopp *et al.* [CLEO Collab.], *Phys. Rev.* **D63**, 092001 (2001).

[8] H. Muramatsu *et al.* [CLEO Collab.], *Phys. Rev. Lett.* **89**, 251802 (2002); Erratum *Phys. Rev. Lett.* **90**, 059901 (2003).

[9] A. Giri, Yu. Grossman, A. Soffer, J. Zupan, *Phys. Rev.* **D68**, 054018 (2003).

[10] A. Bondar, T. Gershon, P. Krokovny, *Phys. Lett.* **B624**, 1 (2005) [`hep-ph/0503174`].

[11] E.P. Wigner, *Phys. Rev.* **70**, 15 (1946).
[12] S.U. Chung *et al.*, *Ann. Phys.* **4**, 404 (1995).
[13] I.J.R. Aitchison, *Nucl. Phys.* **A189**, 417 (1972).